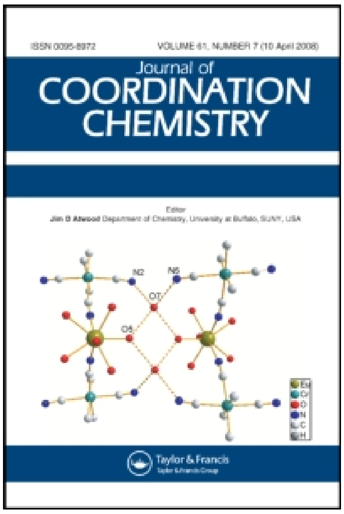

Journal of Coordination Chemistry

Publication details, including instructions for authors and subscription information:
http://www.informaworld.com/smpp/title~content=t713455674

Three new coordination complexes based on 2-methyl-4, 5-imidazoledicarboxylic acid varying from zero- to two-dimensionality

Jiang-Feng Song[ab]; Rui-Sha Zhou[a]; Tuo-Ping Hu[a]; Zhuo Chen[a]; Biao-Bing Wang[b]
[a] Department of Chemistry, North University of China, Taiyuan, Shanxi 030051, P.R. China [b] Shanxi Research Center of Engineering Technology for Engineering Plastics, North University of China, Taiyuan, Shanxi 030051, P.R. China

To cite this Article Song, Jiang-Feng , Zhou, Rui-Sha , Hu, Tuo-Ping , Chen, Zhuo and Wang, Biao-Bing(2010) 'Three new coordination complexes based on 2-methyl-4, 5-imidazoledicarboxylic acid varying from zero- to two-dimensionality', Journal of Coordination Chemistry, 63: 24, 4201 — 4214, First published on: 20 November 2010 (iFirst)

To link to this Article: DOI: 10.1080/00958972.2010.535143

URL: http://dx.doi.org/10.1080/00958972.2010.535143

Journal of Coordination Chemistry
Vol. 63, No. 24, 20 December 2010, 4201–4214

Taylor & Francis
Taylor & Francis Group

Three new coordination complexes based on 2-methyl-4, 5-imidazoledicarboxylic acid varying from zero- to two-dimensionality

JIANG-FENG SONG*†‡, RUI-SHA ZHOU†, TUO-PING HU†,
ZHUO CHEN† and BIAO-BING WANG‡

†Department of Chemistry, North University of China, Taiyuan, Shanxi 030051, P.R. China
‡Shanxi Research Center of Engineering Technology for Engineering Plastics,
North University of China, Taiyuan, Shanxi 030051, P.R. China

(*Received 20 July 2010; in final form 1 October 2010*)

Reaction of 2-methyl-imidazole-4,5-dicarboxylic acid (H_3MIDC) with different salts (Zn and Mn) has led to three new H_nMIDC–metal complexes varying from zero- to two-dimensional structures under hydrothermal and solvothermal conditions. The complex $[Zn(H_2MIDC)_2(H_2O)_2]$ (**1**) is a 0-D complex constructed by H_2MIDC^- and Zn centers and the complex $[Mn(HMIDC)(H_2O)_2] \cdot H_2O$ (**2**) is a polymeric 1-D chiral chain constructed by $HMIDC^{2-}$ and Mn centers connected into a 3-D supramolecular framework with a 1-D channel. The complex $[Zn_3(MIDC)_2(H_2O)_2(DMF)_2] \cdot 0.5H_2O$ (**3**) shows a 2-D puckered structure composed of $MIDC^{3-}$ and Zn. The differences of the three complexes demonstrate that reaction solvent and temperature have important effects on the structure of these complexes. Complex **3** shows strong fluorescence in the solid state at room temperature.

Keywords: 2-Methyl-imidazole-4,5-dicarboxylic acid; Coordination complex; Crystal structure; Fluorescence

1. Introduction

Coordination polymers have intriguing structures and wide potential applications as functional materials [1–9]. Rational design and synthesis of coordination polymers with unique structure and function remain a long-term challenge. Self-assembly of coordination polymers is influenced by medium, pH, temperature, the nature of metal ions, coordination geometry, stereochemistry, and number of coordination donors provided by ligands [10–16]. The pH of solution has had a large impact on the building of coordination polymers with novel structures, for example, imidazole-4,5-dicarboxylic acid (H_3IDC), which can be partially or fully deprotonated to generate H_2IDC^-, $HIDC^{2-}$, and IDC^{3-} anions at different pH values, coordinating with metal ions to form different MOFs with interesting 0-D, 1-D, 2-D, and 3-D topologies [17–26].

---

*Corresponding author. Email: jfsong0129@gmail.com

Journal of Coordination Chemistry
ISSN 0095-8972 print/ISSN 1029-0389 online
DOI: 10.1080/00958972.2010.535143

Over the past few years, extensive investigation has focused on the construction of coordination polymers using 4,5-imidazoledicarboxylic acid as bridges of interest for the following reasons: (1) they are especially good multidentate N- or O-donors with various coordination modes to metal ions and the ability to act as H-bond acceptors and donors to assemble various supramolecular structures; (2) they can be partly or fully deprotonated dependent on the pH, providing various acid–base type coordination modes; (3) the two nitrogens in the imidazole ring can orient the coordination, consistent with Si–O–Si bond angles in zeolites or M–IM–M bond angle in zeolitic imidazolate frameworks (ZIF) [27, 28]. As a derivative of H_3IDC, 2-methyl-imidazole-4,5-dicarboxylic acid (H_3MIDC) is similar with H_3IDC. However, coordination polymers with H_3MIDC are still rare, and only one 3-D (Cd) and six 0-D complexes (Mg, Ni, Co, Mn, Ni, and Ir) based on 2-methyl-4,5-imidazoledicarboxylic acid have been reported [29–36]. Here, three new coordination complexes, $[Zn(H_2MIDC)_2(H_2O)_2]$ (**1**), $[Mn(HMIDC)(H_2O)_2] \cdot H_2O$ (**2**) and $[Zn_3(MIDC)_2(H_2O)_2(DMF)_2] \cdot 0.5H_2O$ (**3**), were obtained under hydrothermal and solvothermal conditions. Only the 0-D complex **1** was obtained under hydrothermal conditions; however, **2** containing 1-D zig-zag chain and **3** with 2-D puckered layer were obtained under solvothermal conditions.

2. Experimental

2.1. *Materials and methods*

All chemicals and solvents were of reagent grade and were used without purification except H_3MIDC, which was prepared according to a literature procedure [37]. Elemental analyses (C, H, and N) were performed on a Perkin Elmer 240C elemental analyzer. Infrared (IR) spectrum was measured on a Perkin Elmer Spectrum One FT-IR spectrometer using KBr pellets. Thermogravimetric analysis (TGA) was performed on a Perkin Elmer TGA-7000 thermogravimetric analyzer under flowing air at a temperature ramp rate of $10^{\circ}C\,min^{-1}$. Fluorescence spectrum was obtained on a LS 55 fluorescence/phosphorescence spectrophotometer at room temperature.

2.2. *Syntheses of 1–3*

2.2.1. Synthesis of 1. A solution of H_3MIDC (8.5 mg, 0.05 mmol) in 5 mL water containing triethylamine (28 µL, 2 mmol) was directly mixed with a solution of $ZnCl_2 \cdot 4H_2O$ in 1 mL water ($0.10\,mol\,L^{-1}$) at room temperature in a 15 mL beaker; HNO_3 ($3\,mol\,L^{-1}$) was added until the mixture became clear. The resulting colorless solution was transferred and sealed in a 25 mL Teflon-lined stainless steel reactor, and heated at 150°C for 72 h. Upon cooling to room temperature, colorless crystals were filtered and washed with water and ethanol. Yield: 85% (based on H_3MIDC). Elemental Anal. Calcd $C_{12}H_{12}N_4O_{10}Zn$ (431.19): C, 33.40; H, 2.78; and N, 12.99. Found: C, 33.43; H, 2.82; and N, 12.34. IR data (KBr, cm^{-1}): (w = weak, m = medium, s = strong). 3245(m), 3114(m), 2944(w), 1605(s), 1538(s), 1413(s), 1250(m), 1090(s), 1005(m), 866(m), 790(s), and 694(m).

2.2.2. Synthesis of 2. A solution of H_3MIDC (8.5 mg, 0.05 mmol) in 5 mL DMF containing triethylamine (28 µL, 2 mmol) was mixed with a solution of $MnCl_2 \cdot 4H_2O$ in 1 mL H_2O (0.10 mol L^{-1}) at room temperature in a 15 mL beaker; HNO_3 (3 mol L^{-1}) was added until the mixture became clear. The resulting colorless solution was transferred and sealed in a 25 mL Teflon-lined stainless steel reactor, and heated at 85°C for 72 h. Upon cooling to room temperature, colorless crystals were filtered and washed with DMF and ethanol. Yield: 70% (based on H_3MIDC). Elemental Anal. Calcd $C_6H_{10}MnN_2O_7$ (277.1): C, 25.98; H, 3.61; and N, 10.10. Found: C, 26.04; H, 3.55; and N, 10.15. IR data (KBr, cm^{-1}): 3310(m), 3106(m), 2947(w), 1599(s), 1518(s), 1413(s), 1087(s), 1005(m), 866(m), 788(s), and 694(m).

2.2.3. Synthesis of 3. The procedure was the same as that for **2** except that $MnCl_2 \cdot 4H_2O$ was replaced by $ZnCl_2 \cdot 4H_2O$ (0.10 mol L^{-1}). Yield: 58% (based on H_3MIDC). Elemental Anal. Calcd $C_{18}H_{25}N_6O_{12.5}Zn_3$ (721.55): C, 29.94; H, 3.46; and N, 11.64. Found: C, 30.01; H, 3.39; and N, 11.67. IR data (KBr, cm^{-1}): 3415(w), 1602(s), 1510(s), 1358(s), 1068(m), 739(s), and 628(m).

2.3. *Crystal structure determination*

The crystal structures were determined by single-crystal X-ray diffraction. Reflection data were collected on a Bruker SMART CCD area-detector diffractometer (Mo-Kα radiation, graphite monochromator) at room temperature with ω-scan mode. Empirical adsorption corrections were applied to all data using SADABS. The structures were solved by direct methods and refined by full-matrix least squares on F^2 using SHELXTL 97 software [38]. Non-hydrogen atoms were refined anisotropically. Hydrogens were located from difference Fourier maps refined as riding, with O–H = 0.85, N–H = 0.85 in **1**–**3**. All calculations were carried out using SHELXTL 97 [38] and PLATON [39]. Crystallographic data and pertinent information are given in table 1; selected bond lengths and angles in table 2, and geometric parameters of hydrogen bonds in table 3.

3. Results and discussion

3.1. *Synthesis*

In order to obtain the complexes based on H_3MIDC, we attempted experiments under hydrothermal and solvothermal conditions. The reactions were conducted in the same mole ratio of metal-to-ligand ($H_3MIDC/M^{2+} = 1:1$) under hydrothermal conditions (150°C) at different pH values (5–8). The 0-D complexes containing different metal ions, which are isomorphic with **1**, were easily obtained under hydrothermal conditions; however, the complexes with high dimensions were difficult to obtain. Yield may depend on the pH of reaction system, but the reaction was not significantly affected by pH (5–8). Highest yields were achieved when pH values of the solutions are equal to 6, namely, the amount of triethylamine is 28 µL. Only, unidentified powders were obtained when the final pH values are over 8; however, only H_3MIDC was obtained

Table 1. Crystal and structure refinement data for **1**–**3**.

Complex	**1**	**2**	**3**
Empirical formula	$C_{12}H_{12}N_4O_{10}Zn$	$C_6H_{10}MnN_2O_7$	$C_{18}H_{25}N_6O_{12.5}Zn_3$
Formula weight	431.19	277.10	720.54
Crystal system	Orthorhombic	Monoclinic	Monoclinic
Space group	*Pbca*	*P*2(1)/*n*	*C*2/*c*
Unit cell dimensions (Å, °)			
a	6.7541(9)	10.6865(14)	16.5509(16)
b	13.8980(18)	7.8570(10)	10.4657(10)
c	16.702(2)	12.5255(16)	16.1639(15)
α	90	90	90
β	90	105.391(2)	104.631(2)
γ	90	90	90
Volume (Å^3), *Z*	1567.8(3), 4	1014.0(2), 4	2709.1(4), 4
Calculated density (g cm^{-3})	1.827	1.815	1.767
Absorption coefficient (mm^{-1})	1.163	1.326	2.706
Crystal size (mm^3)	0.33 × 0.20 × 0.12	0.24 × 0.18 × 0.15	0.25 × 0.20 × 0.10
θ range for data collection (°)	2.44–26.10	2.23–26.17	2.32–26.03
Reflections collected	7989	5401	7360
Independent reflection	1559 [$R(\text{int}) = 0.0243$]	2011 [$R(\text{int}) = 0.0239$]	2660 [$R(\text{int}) = 0.0521$]
Completeness	99.9%	99.1%	99.8%
Goodness-of-fit on F^2	1.080	1.248	0.987
Final *R* indices [$I > 2\sigma(I)$]^a	$R_1 = 0.0325$, $wR_2 = 0.0958$	$R_1 = 0.0429$, $wR_2 = 0.1037$	$R_1 = 0.0434$, $wR_2 = 0.1005$
R indices (all data)^a	$R_1 = 0.0404$, $wR_2 = 0.1013$	$R_1 = 0.0465$, $wR_2 = 0.1053$	$R_1 = 0.0704$, $wR_2 = 0.1139$

$^aR_1 = \Sigma||F_o| - |F_c||/\Sigma|F_o|$; $wR_2 = [\Sigma w(F_o^2 - F_c^2)_2/\Sigma w(F_o^2)^2]^{1/2}$.

when the final pH values are less than 5. Keeping the same mole ratio of metal-to-ligand and triethylamine (28 µL), **2** and **3** were obtained with mixed DMF/H_2O. The possible reasons are: (1) the main form is H_2MIDC^- under hydrothermal conditions; however, $HMIDC^{2-}$ or $MIDC^{3-}$ increased under solvothermal conditions; (2) compared with H_2MIDC^-, $HMIDC^{2-}$ or $MIDC^{3-}$, is a stronger coordinator with more coordination sites, improving coordination with M^{n+} into high-dimension topologies; (3) solvents play an important role in the removal of the three hydrogens of H_3MIDC; (4) as the temperature increases, the decomposition rate of DMF will increase, resulting in the formation of base and insoluble solid. So, the lower temperature is helpful to obtain good crystals easily characterized by X-ray single crystal diffractions.

3.2. *Crystal structure*

3.2.1. Crystal structure of 1. X-ray crystallography reveals that **1** is isomorphous to previously reported complexes constructed by the first-transition metal (Ni, Co, Cd, and Mn) and H_2MIDC^- [30–33]. Complex (**1**) is composed of one Zn(II), two mono-deprotonated H_2MIDC^-, and two coordination waters (figure 1). The Zn, with a slightly distorted octahedral geometry where the basal plane is occupied by two carboxylate oxygens (O1 and O1a, symmetry code: *a*, $1-x$, $1-y$, $-z$) and two nitrogens (N1 and N1a) from two chelating H_2MIDC^- ligands, lies on a crystallographic inversion center; the axes are occupied by two waters. The bond angles around Zn are *ca* 90° and 180°; bond lengths and angles are given in table 2. In H_2MIDC^-, an intramolecular hydrogen bond with an O $\cdots$ O distance of 2.455(2) Å (O2 and O3) is

Table 2. Bond lengths (Å) and angles (°) for **1**–**3**.

1			
Zn(1)–O(1W)	2.0622(9)	N(1)#1–Zn(1)–N(1)	180.00(9)
Zn(1)–N(1)	2.0750(9)	O(1W)–Zn(1)–O(1)#1	91.91(7)
Zn(1)–O(1)	2.2442(6)	O(1W)–Zn(1)–O(1)	88.09(7)
O(1W)–Zn(1)–O(1W)#1	180.0	N(1)#1–Zn(1)–O(1)	102.30(7)
O(1W)–Zn(1)–N(1)#1	88.21(7)	N(1)–Zn(1)–O(1)	77.70(7)
O(1W)–Zn(1)–N(1)	91.79(7)	O(1)#1–Zn(1)–O(1)	180.00(8)
2			
Mn(1)–O(2W)	2.149(3)	O(3)#2–Mn(1)–O(1)	91.89(9)
Mn(1)–O(2)#2	2.156(3)	O(2W)–Mn(1)–O(1W)	87.26(1)
Mn(1)–O(3)#2	2.168(2)	O(2)#2–Mn(1)–O(1W)	87.47(1)
Mn(1)–O(1)	2.182(2)	O(3)#2–Mn(1)–O(1W)	93.35(1)
Mn(1)–O(1W)	2.200(3)	O(1)–Mn(1)–O(1W)	174.76(1)
Mn(1)–N(1)	2.231(3)	O(2W)–Mn(1)–N(1)	97.14(1)
O(2W)–Mn(1)–O(2)#2	167.84(10)	O(2)#2–Mn(1)–N(1)	94.62(10)
O(2W)–Mn(1)–O(3)#2	86.60(10)	O(3)#2–Mn(1)–N(1)	165.81(10)
O(2)#2–Mn(1)–O(3)#2	82.77(10)	O(1)–Mn(1)–N(1)	74.26(10)
O(2W)–Mn(1)–O(1)	93.57(10)	O(1W)–Mn(1)–N(1)	100.51(1)
O(2)#2–Mn(1)–O(1)	92.70(10)		
3			
Zn(1)–O(4)	2.012(3)	O(4)–Zn(1)–O(5)	88.63(3)
Zn(1)–O(2)	2.089(3)	O(2)–Zn(1)–O(5)	89.45(3)
Zn(1)–O(5)	2.119(3)	O(5)#3–Zn(1)–O(5)	180.00(8)
Zn(2)–O(1W)	1.985(3)	O(1W)–Zn(2)–N(2)	118.89(5)
Zn(2)–N(2)	2.012(4)	O(1W)–Zn(2)–N(3)#4	123.97(5)
Zn(2)–N(3)#4	2.024(4)	N(2)–Zn(2)–N(3)#4	117.05(5)
Zn(2)–O(1)#4	2.076(3)	O(1W)–Zn(2)–O(1)#4	92.17(5)
Zn(2)–O(3)	2.140(3)	N(2)–Zn(2)–O(1)#4	101.31(3)
O(4)–Zn(1)–O(4)#3	180.0	N(3)#3–Zn(2)–O(1)#4	80.32(3)
O(4)–Zn(1)–O(2)#3	85.95(2)	O(1W)–Zn(2)–O(3)	89.19(4)
O(4)–Zn(1)–O(2)	94.07(2)	N(2)–Zn(2)–O(3)	79.52(3)
O(2)#3–Zn(1)–O(2)	180.00(9)	N(3)#4–Zn(2)–O(3)	97.54(3)
O(4)–Zn(1)–O(5)#3	91.39(3)	O(1)#4–Zn(2)–O(3)	177.85(2)
O(2)–Zn(1)–O(5)#3	90.57(3)		

Symmetry transformations used to generate equivalent atoms: #1: $-x+1, -y+1, -z$; #2: $-x+1/2, y-1/2, -z+1/2$; #3: $-x, -y+2, -z$; #4: $-x+1/2, y-1/2, -z+1/2$.

formed between the carboxyl and carboxylate groups. In **1**, H_2MIDC^- coordinates with Zn(II) in a N, O-chelating mode to form a five-membered ring, as shown in scheme 1(a).

Each water in **1** is involved in two intermolecular O–H ··· O hydrogen bonds with two uncoordinated O3 and O4 from two neighboring molecules to generate a 2-D supramolecular structure (figure 2), in which two waters and two carboxyl groups form an eight-membered ring. The 2-D supramolecular layers are joined into a 3-D supramolecular network through N–H ··· O hydrogen bonds (N2–H4 ··· O2) between the imidazole nitrogen that is not coordinating to Zn and carboxyl group (figure 3); the geometric parameters of hydrogen bonds are given in table 3.

3.2.2. Crystal structure of 2.

The asymmetric unit of **2** contains a Mn(II), a μ_2-$HMIDC^{2-}$, two coordinated waters, and a lattice water (figure 4). Each Mn is a distorted octahedral where the basal plane (with the largest deviation 0.2409 Å (O2w)) is

Table 3. Hydrogen bonds for **1**–**3**.

D–H···A	d(D–H)	d(H···A)	d(D···A)	∠DHA
1				
N2–H4···O2#1	0.868	2.085	2.934	165.70
O1w–H1wb···O3#2	0.864	1.935	2.776	167.59
O1w–H1wa···O4#3	0.868	1.904	2.767	173.32
O3–H5···O2	0.857	1.602	2.455	173.49
2				
N2–H1···O2#4	0.860	2.110	2.916	155.66
O1w–H1wa···O4#5	0.847	2.212	2.963	147.76
O1w–H1wb···O4#6	0.846	2.028	2.873	176.51
O2w–H2wa···O3#6	0.851	1.843	2.693	176.66
O2w–H2wb···O3w	0.853	1.867	2.710	169.40
O3w–H3wa···O4#7	0.848	2.096	2.926	165.94
3				
O1w–H2wa···O3#8	0.850	2.026	2.857	165.35
O1w–H1wa···O2#9	0.847	1.938	2.775	169.60

Symmetry codes: #1: $-x+1, y-1/2, -z+1/2$; #2: $x-1/2, y, -z+1/2$; #3: $-x+1/2, -y+1, z-1/2$; #4: $x+1/2, -y+1/2, z+1/2$; #5: $-x+1, -y, -z+1$; #6: $x+1/2, -y+1/2, z-1/2$; #7: $-x+1, -y+1, -z+1$; #8: $-x+1/2, -y+3/2, -z$; #9: $x+1/2, y-1/2, z$.

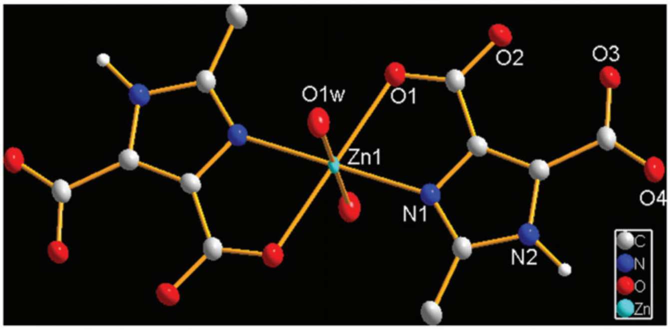

Figure 1. The coordination environment of Zn in **1**. Thermal ellipsoids are at 50% probability.

occupied by two carboxylate oxygens (O2 and O3) and a nitrogen (N1) from two equivalent HMIDC^{-} ligands with one coordinated water (O2w); the axes are occupied by one coordinated water (O1w) and one carboxylate oxygen (O1a) from HMIDC^{2-}. The Mn–L (L = O, N) bond distances are in the range 2.149(3)–2.231(3) Å and the L–Mn–L bond angles are in the range 74.26(10)–174.75(11)°. These angles further confirm the distorted octahedral geometry of Mn(II) in **2**. The HMIDC^{2-} coordinates with Mn(II) in a N,O-chelating mode to form a five-membered ring and a O,O-chelating mode to form a seven-membered ring. The N,O-chelating and O,O-chelating coordination of HMIDC^{2-} are shown in scheme 1(b), which is similar to that of 4,5-dicarboxy-imidazole (Hdcbi^{2-}) in [Mn(Hdcbi)(H_2O)] [40]. Though they have similar coordination of Hdcbi^{2-} and HMIDC^{2-}, completely different topology structures were obtained. The Mn centers are connected into a 2-D layer in [Mn(Hdcbi)(H_2O)] [40]; however, a 1-D chiral chain is constructed by HMIDC^{2-} anions and Mn centers in **2**.

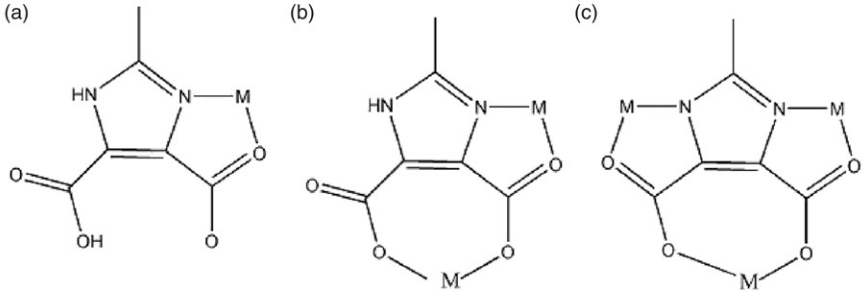

Scheme 1. Coordination modes of H_nMIDC.

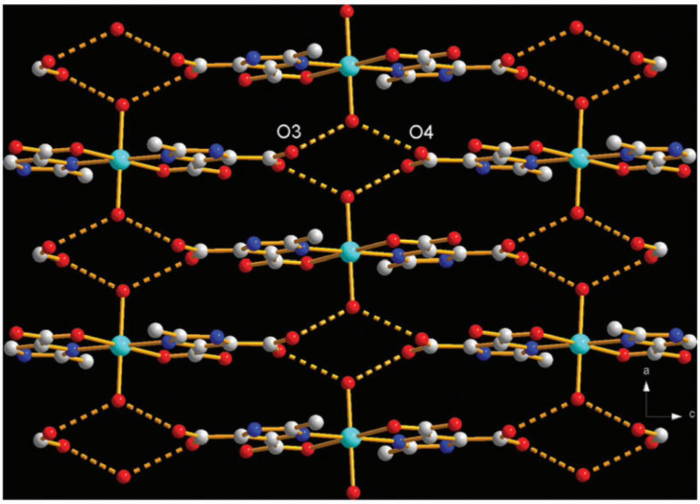

Figure 2. The 2-D supramolecular structure constructed by O–H $\cdots$ O hydrogen bonds in **1**.

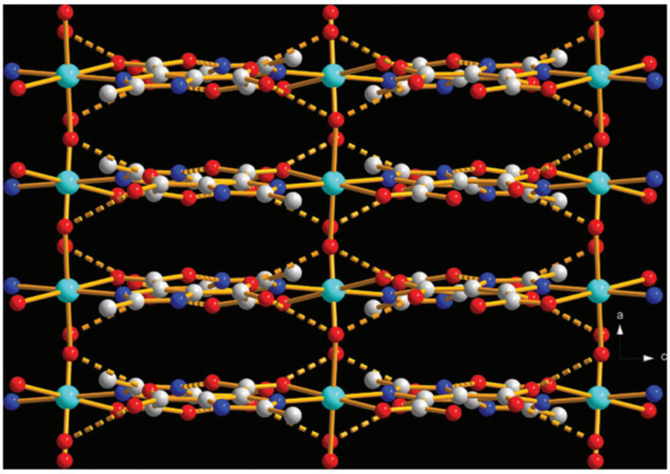

Figure 3. The 3-D supramolecular network constructed by O–H $\cdots$ O and N–H $\cdots$ O hydrogen bonds in **1**.

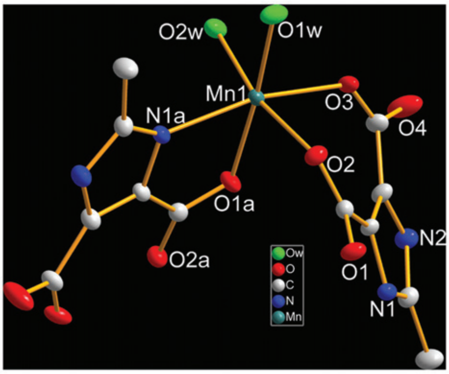

Figure 4. The coordination environment of Mn center in **2**. Thermal ellipsoids are at 50% probability.

Each μ_2-HMIDC^{2-} connects two Mn(II) ions into a chiral chain with a helical pitch of 7.8570(13) Å, as shown in figure 5(a). The 1-D chiral chains are connected into a 2-D supramolecular layer with square-grid framework through O–H$\cdots$O hydrogen bonds between coordinated water (O1w) and the uncoordinated oxygens (O4) of carboxyl groups of HMIDC^{2-}. The square-grid has six Mn(II) and four HMIDC^{2-}. The lattice waters are located in the square-grid through O–H$\cdots$O hydrogen bonds between coordinated water (O2w) and lattice water (O3w) (figure 5b). The 2-D layers are further connected into a 3-D supramolecular network with a 1-D channel containing lattice water through O–H$\cdots$O and N–H$\cdots$O hydrogen bonds among adjacent chains (figure 6). O1w links two symmetry equivalent oxygens (O4) from two different adjacent chains (O1w–H1wa$\cdots$O4 and O1w–H1wb$\cdots$O4).

3.2.3. Crystal structure of 3. The asymmetric unit of **3** contains half a Zn1, a Zn2 ion, a μ_3-MIDC^{3-}, a coordinated DMF, 0.25 lattice water, and a coordinated water (figure 7). Zn1 is located on an inversion center and displays different coordination environment and geometry from Zn2. Each Zn1 is coordinated with four oxygens (O2, O4, O2a, and O4a) from two symmetry-equivalent μ_3-MIDC^{3-} in the equatorial plane, and two symmetry-equivalent DMF molecules in axial positions forming a slightly distorted octahedron. The axial Zn–O bond distance (d(Zn1–O5) = 2.119(3) Å) is slightly longer than the equatorial Zn–O bond distances (d(Zn1–O2) = 2.012(3) and d(Zn1–O4) = 2.089(3) Å). The bond angles around Zn1 center are *ca* 90° and 180°, indicating slight distortion of the Zn1 octahedral geometry. Each Zn2 is a distorted square pyramid with two oxygens (O1a and O3, symmetry code: a, $0.5 - x$, $-0.5 + y$, $0.5 - z$) and two nitrogens (N2 and N3a) from three symmetry equivalent μ_3-MIDC^{3-} in the equatorial plane, and the axial position is occupied by one water. The axial Zn–Ow bond distance (1.985(3) Å) is slightly shorter than the equatorial Zn–O and Zn–N bond distances. The O/N–Zn–O/N bond angles around Zn2 range from 79.51(13) to 177.84(12)°, indicating distortion of the Zn2 square pyramid; the corresponding bond lengths and angles are given in table 2. In **3**, MIDC^{3-} coordinates with Zn(II) μ_3-hexadentate to form two five-membered rings and a seven-membered ring, as shown in scheme 1(c). Though some complexes based on IDC^{3-} in μ_3-hexadentate mode have

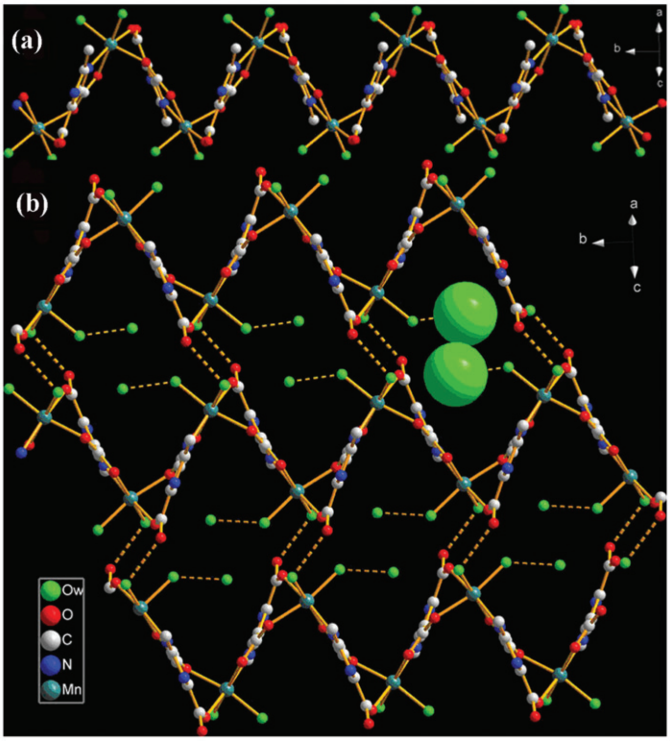

Figure 5. (a) The 1-D chiral chain constructed by Mn center and $HMIDC^-$; (b) the 1-D chiral chains are connected into a 2-D supramolecular layer with square-grid in **2**.

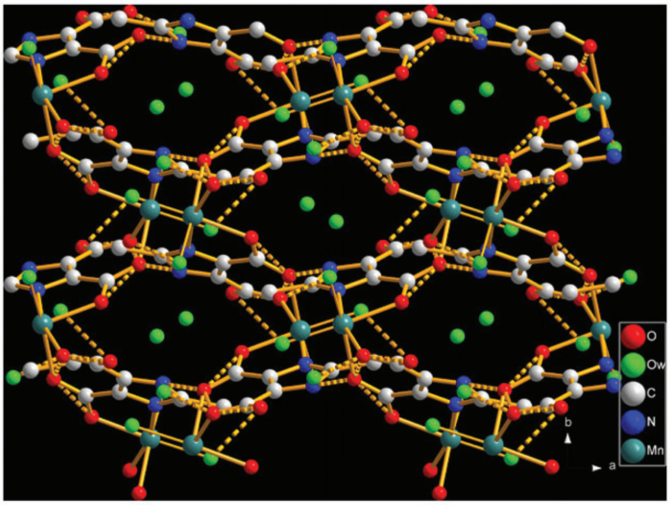

Figure 6. The 3-D supramolecular network with 1-D channels through O–H $\cdots$ O and N–H $\cdots$ O hydrogen bonds in **2**.

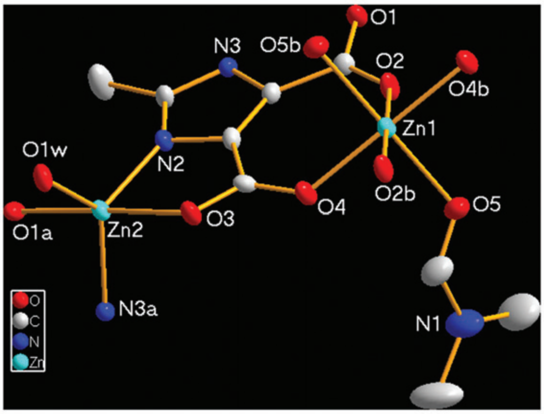

Figure 7. The coordination environment of Zn1 and Zn2 in **3**. Thermal ellipsoids are at 50% probability.

been reported [41, 42], the topology structures constructed by IDC^{3-} and metal ions were different from that of **3**. We found a 2-D layer topology structure in $\{[Zn_3(IDC)_2(bpy)_3]\cdot(bpy)\cdot(H_2O)_8\}_n$ and $\{[Co_3(IDC)_2(4,4'\text{-bipy})_3]\cdot 6H_2O\cdot DMF\}_n$ [bpy = 4,4′-bipy], constructed by the 2-D honeycomb-like sheets of $[M_3(IDC)_2]_n$, similar with 2-D layer of **3** and μ-2 bpy bridges.

Each μ_3-$MIDC^{3-}$ connects three Zn(II) ions into a 2-D wavelike layer with (3, 6) topology along the *a*-axis, as illustrated in figure 8(a), in which 3-connected nodes and 2-connected connectors are provided by $MIDC^{3-}$ and Zn(II), respectively (figure 8b). Coordinated DMF molecules lie on two sides of the 2-D layer in an anti-parallel fashion. At the wave crest and trough of the 2-D wavelike layer, the coordinated waters (O1w) are hydrogen bond donors. The 2-D puckered layers were connected into a 3-D supramolecular network with a 1-D hexagonal channel of $10.5\times 11.0\,\text{Å}^2$ in which terminal DMF ligands protrude through the O–H···O hydrogen bonds between coordinated water molecules (O1w) and the oxygens (O5 and O6) of carboxyl groups of $MIDC^{3-}$ anions (figure 9).

3.3. *The TG curves of 1–3*

The thermal behaviors of **1**–**3** from 25°C to 700°C under air (figure 10) display two weight loss steps. The first of 10.12% of **1**, from 108°C to 197°C, is assigned to loss of water. The second weight loss of 71.59% from 249°C to 647°C corresponds to decomposition of the organic component. The total weight loss of **1** is 81.71% (Calcd 81.12%). For **2**, the first weight loss of 16.98% at 61–165°C is attributed to loss of coordination and lattice water. The second weight loss of 51.32% from 330°C to 431°C corresponds to decomposition of the organic component. The total weight loss of **2** is 73.17% (Calcd 74.38%). For **3**, the first loss of 23.82% from 132°C to 299°C corresponds to loss of lattice water, coordinated water, and part of DMF. The second weight loss (41.82%) from 299°C and 548°C is characteristic of combustion of the remaining DMF and MIDC. The total weight loss of **3** amounts to 65.64% (Calcd 66.18%).

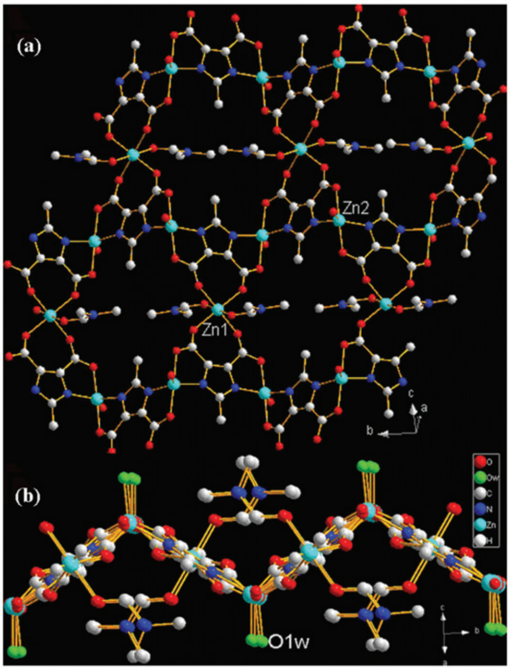

Figure 8. (a) The 2-D layer constructed by μ_3–MIDC^{3-} anions and Zn(II) ions; (b) the 2-D wavelike layer in **3**.

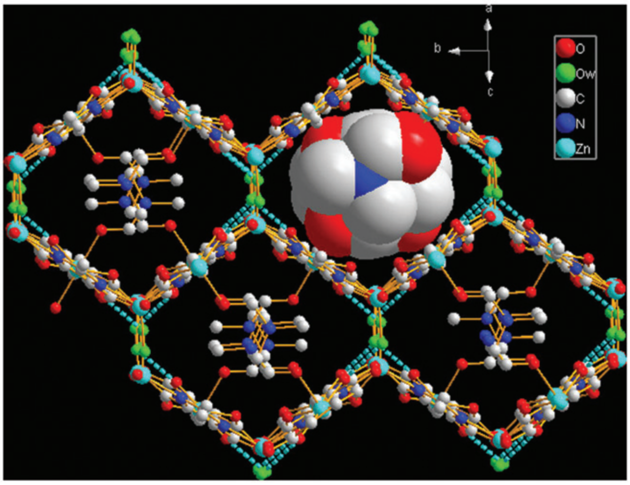

Figure 9. The 3-D supramolecular network with a 1-D hexagonal channel of 10.5 × 11.0 Å^2 in **3**.

3.4. *The fluorescence curve of 3*

The solid-state fluorescence spectrum of **3** is shown in figure 11. In order to understand the nature of the emission band, the luminescence of H_3MIDC in solid state was also investigated at room temperature. Free H_3MIDC luminescence cannot be detected in

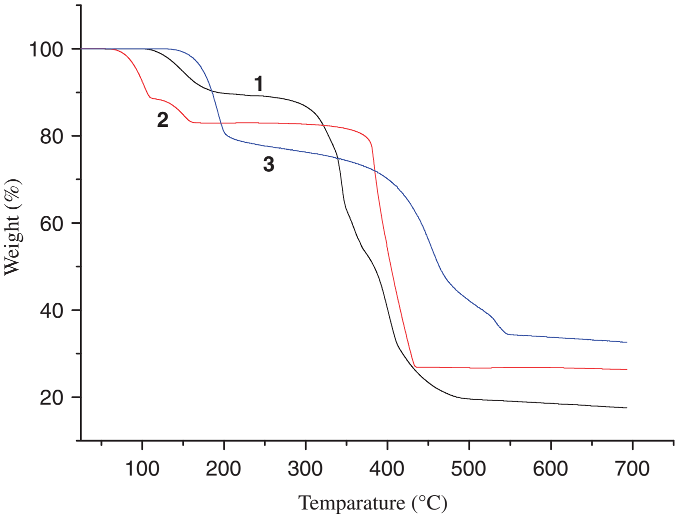

Figure 10. The TGA curves of **1–3**.

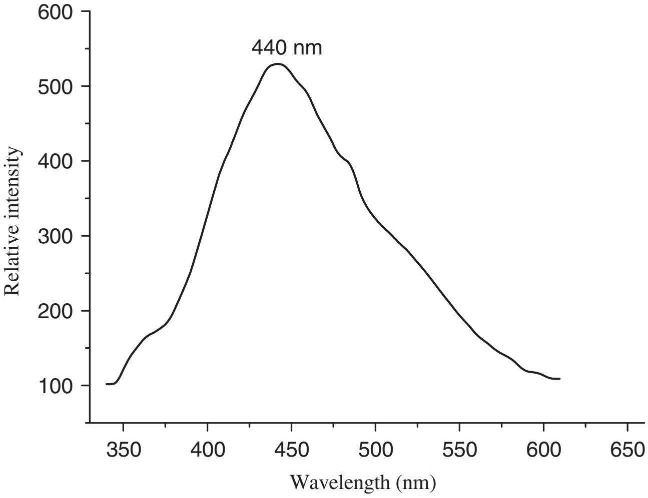

Figure 11. The emission spectrum of **3** at room temperature.

solid state at ambient temperature upon excitation at 320 nm. Complex **3** exhibits intense blue photoluminescence with maximum emission *ca* 440 nm upon excitation at 320 nm. Previous study revealed that if the ligand is a heterocylic aromatic, the heteroatom can effectively decrease the π and π^* orbital energies. Thus, the HOMO and LUMO of the complexes may lack the contribution from metal atoms, and the ligand-to-metal charge transfer emission can be excluded [40]. Thus, the emission band of **3** might be assigned to ligand-centered $\pi^* \to \pi$ emission, similar to that of Zn complexes [43, 44].

4. Conclusion

In this study, H_3MIDC with Zn and Mn salts led to three new H_nMIDC-metal complexes. The complex $[Zn(H_2MIDC)_2(H_2O)_2]$ (**1**) is a 0-D complex constructed by H_2MIDC^- and Zn. The complex $[Mn(HMIDC)(H_2O)_2] \cdot H_2O$ (**2**) with a polymeric 1-D chiral chain constructed by $HMIDC^{2-}$ and Mn is connected into a 3-D supramolecular framework with a 1-D channel. $[Zn_3(MIDC)_2(H_2O)_2(DMF)_2] \cdot 0.5H_2O$ (**3**) shows a 2-D puckered structure composed of $MIDC^{3-}$ anions and Zn ions. Analyses of synthetic conditions, structures, and coordination modes of H_nMIDC reveal that the solvent and temperature have important effects on the structure of these complexes and coordination modes of H_nMIDC. This study reveals that new coordination polymers with high dimensionality will be synthesized using H_3MIDC or its derivatives as building units. Further research for construction of new architectures with other transition metals is underway in our laboratory.

Supplementary materials

CCDC 783131–783133 for **1**–**3** contain the supplementary crystallographic data. These data can be obtained free of charge from The Cambridge Crystallographic Data Centre *via* http://www.ccdc.cam.ac.uk/data_request/cif.

Acknowledgments

This study was supported by the Natural Science Young Scholars Foundation of North University of China and the Scientific Research Start-up Foundation of North University of China.

References

[1] M. Eddaoudi, D.B. Moler, H.L. Li, B.L. Chen, T.M. Reineke, M. O'Keeffe, O.M. Yaghi. *Acc. Chem. Res.*, **34**, 319 (2001).
[2] B.J. Holliday, C.A. Mirkin. *Angew. Chem., Int. Ed.*, **40**, 2022 (2001).
[3] B. Moulton, M.J. Zaworotko. *Chem. Rev.*, **101**, 1629 (2001).
[4] O.M. Yaghi, M. O'Keeffe, N.W. Ockwig, H.K. Chae, M. Eddaoudi, J. Kim. *Nature*, **423**, 705 (2003).
[5] S. Kitagawa, R. Kitaura, S. Noro. *Angew. Chem., Int. Ed.*, **43**, 2334 (2004).
[6] G. Ferey. *Chem. Soc. Rev.*, **37**, 191 (2008).
[7] J.R. Li, R.J. Kuppler, H.C. Zhou. *Chem. Soc. Rev.*, **38**, 1477 (2009).
[8] L.Q. Ma, C. Abney, W.B. Lin. *Chem. Soc. Rev.*, **38**, 1248 (2009).
[9] D.J. Tranchemontagne, J.L. Mendoza-Cortes, M. O'Keeffe, O.M. Yaghi. *Chem. Soc. Rev.*, **38**, 1257 (2009).
[10] T.L. Hennigar, D.C. MacQuarrie, P. Losier, R.D. Rogers, M.J. Zaworotko. *Angew. Chem., Int. Ed.*, **36**, 972 (1997).
[11] A.J. Blake, N.R. Brooks, N.R. Champness, P.A. Cooke, A.M. Deveson, D. Fenske, P. Hubberstey, W.S. Li, M. Schroder. *J. Chem. Soc., Dalton Trans.*, 2103 (1999).
[12] C.Y. Su, Y.P. Cai, C.L. Chen, M.D. Smith, W. Kaim, H.C.Z. Zoye. *J. Am. Chem. Soc.*, **125**, 8595 (2003).

[13] S.C. Chen, Z.H. Zhang, K.L. Huang, Q. Chen, M.Y. He, A.J. Cui, C. Li, Q. Liu, M. Du. *Cryst. Growth Des.*, **8**, 3437 (2008).
[14] B.R. Manzano, F.A. Jalon, M.L. Soriano, M.C. Carrion, M.P. Carranza, K. Mereiter, A.M. Rodriguez, A. de la Hoz, A. Sanchez-Migallon. *Inorg. Chem.*, **47**, 8957 (2008).
[15] T.K. Prasad, M.V. Rajasekharan. *Cryst. Growth Des.*, **8**, 1346 (2008).
[16] G.J.T. Cooper, G.N. Newton, D.L. Long, P. Kogerler, M.H. Rosnes, M. Keller, L. Cronin. *Inorg. Chem.*, **48**, 1097 (2009).
[17] J.Y. Lu, Z.H. Ge. *Inorg. Chim. Acta*, **358**, 828 (2005).
[18] T.K. Maji, G. Mostafa, H. Chang, S. Kitagawa. *Chem. Commun.*, 2436 (2005).
[19] P. Mahata, S. Natarajan. *Eur. J. Inorg. Chem.*, 2156 (2005).
[20] W.G. Lu, C.Y. Su, T.B. Lu, L. Jiang, J.M. Chen. *J. Am. Chem. Soc.*, **128**, 34 (2006).
[21] R.Q. Zou, H. Sakurai, Q. Xu. *Angew. Chem., Int. Ed.*, **45**, 2542 (2006).
[22] Y.Q. Sun, G.Y. Yang. *Dalton Trans.*, 3771 (2007).
[23] W.G. Lu, J.Z. Gu, L. Jiang, M.Y. Tan, T.B. Lu. *Cryst. Growth Des.*, **8**, 986 (2008).
[24] C.F. Wang, E.Q. Gao, Z. He, C.H. Yan. *Chem. Commun.*, 720 (2004).
[25] R.Q. Fang, X.M. Zhang. *Inorg. Chem.*, **45**, 4801 (2006).
[26] S. Wang, L.R. Zhang, G.H. Li, Q.S. Huo, Y.L. Liu. *CrystEngComm*, **10**, 1662 (2008).
[27] R. Banerjee, A. Phan, B. Wang, C. Knobler, H. Furukawa, M. O'Keeffe, O.M. Yaghi. *Science*, **319**, 939 (2008).
[28] B. Wang, A.P. Cote, H. Furukawa, M. O'Keeffe, O.M. Yaghi. *Nature*, **453**, 207 (2008).
[29] Y.L. Li, X. Guo, J.X. Wang, Y.C. Wang. *Acta Cryst.*, **E65**, m772 (2009).
[30] H.L. Wen, B.W. Lai, X.X. Wu, X.L. Nie, X.B. Hu. *Z. Kristallogr. – New Cryst. Struct.*, **224**, 455 (2009).
[31] J.Z. Zeng, X.G. Yi, J.Y. Lin, S.M. Ying, G.S. Huang. *Acta Cryst.*, **E64**, m476 (2008).
[32] X.L. Nie, H.L. Wen, Z.S. Wu, D.B. Liu, C.B. Liu. *Acta Cryst.*, **E63**, m753 (2007).
[33] C.B. Liu, X.L. Nie, H.L. Wen. *Acta Cryst.*, **E63**, m2244 (2007).
[34] G. Net, J.C. Bayon, W.M. Butler, P.R. Smussen. *Chem. Commun.*, 1022 (1989).
[35] S.P. Tang. *Acta Cryst.*, **E65**, m504 (2009).
[36] F.F. Dang, X.W. Wang, G.P. Han, Y.H. Yao. *Monatsh. Chem.*, **140**, 615 (2009).
[37] G. Tsukamoto, K. Yoshino, T. Kohno, H. Ohtaka, H. Kagaya, K. Ito. *J. Med. Chem.*, **23**, 738 (1980).
[38] G.M. Sheldrick. *SHELXS 97, Program for Crystal Structure Refinement*, University of Göttingen, Göttingen, Germany (1998).
[39] A.L. Spek. *PLATON, Molecular Geometry Program*, University of Utrecht, The Netherlands (1999).
[40] R.Q. Fang, X.M. Zhang. *Inorg. Chem.*, **45**, 4801 (2006).
[41] W.G. Lu, L. Jiang, X.L. Feng, T.B. Lu. *Cryst. Growth Des.*, **6**, 564 (2006).
[42] Y.L. Wang, D.Q. Yuan, W.H. Bi, X. Li, X.J. Li, F. Li, R. Cao. *Cryst. Growth Des.*, **5**, 1849 (2005).
[43] S.L. Zheng, X.M. Chen. *Aust. J. Chem.*, **57**, 703 (2004).
[44] S.L. Zheng, J.H. Yang, X.L. Yu, X.M. Chen, W.T. Wong. *Inorg. Chem.*, **43**, 830 (2004).